

2D CO CRS stack for top-surface topography

T. Boelsen

email: Tim.Boelsen@gpi.uni-karlsruhe.de

keywords: CO CRS stack, topography, wavefield attributes, redatuming

ABSTRACT

I present new hyperbolic traveltimes formulas for the 2D Common-Offset (CO) Common-Reflection-Surface (CRS) stack that are able to take top-surface topography into account. I consider two types of topography, namely a rugged topography and a smooth one. The formula for a rugged topography can be used to derive a stacking operator that is in principle able to handle a vertical seismic profile (VSP) acquisition geometry. Moreover, I propose an approach how to perform redatuming of the 2D CO CRS stack section. Finally, I will show the application of the 2D CO CRS stack and the redatuming algorithm to a synthetic data set that was simulated with a smoothly curved measurement surface.

INTRODUCTION

The 2D CRS stack was originally developed to stack pre-stack data acquired along a straight line on a planar measurement surface into a zero-offset (ZO) section (2D ZO CRS stack), see for instance Mann et al. (1999) and Müller (1999). Zhang (2003) derived traveltimes formulas for the 2D ZO CRS stack for an arbitrarily complex top-surface topography and Chira (2001) considered a smooth topography. Zhang et al. (2001) extended the CRS stack for finite-offset (FO), i.e., the pre-stack data are stacked into a FO gather. If this gather is a common-offset (CO) gather, it is referred to as 2D CO CRS stack (Bergler, 2001). Both authors considered planar measurement surfaces only. In this paper, I want to extend the 2D CO CRS stack for top-surface topography.

In addition to a high-quality stacked section (high signal-to-noise ratio), we obtain wavefield attribute sections by the CRS stack that can be used for further analyses. In the presence of top-surface topography, one very attractive application of the attributes is redatuming, i.e., projecting the sources and receivers onto a new horizontal datum line and continuing the wavefield along the central rays until it reaches the datum line. This is done in order to get rid of the topographic influence on the data. Since the emergence angles of the central rays are determined by the CRS stack (one angle in the ZO case and two angles in the CO case), redatuming can be performed in a very accurate way. Zhang (2003) and Heilmann (2002) showed how redatuming can be done in the ZO case.

In this paper, I will propose a method how to perform redatuming for the CO CRS stack and show that it is more complicated than in the ZO case.

SECOND ORDER TRAVELTIME FORMULAS

Zhang (2003) derived the most general moveout formula used in the CRS stack. The following issues can be taken into account by this formula:

- 3D data acquisition on a measurement surface in addition to 2D data acquisition along a straight line.
- An arbitrary top-surface topography since the formula explicitly depends on the source and receiver elevations.
- Velocity gradients in the vicinity of the sources and receivers.

Zhang (2003) used this formula in order to derive stacking operators for the 2D ZO CRS stack in the presence of an arbitrary topography and for the 2D FO CRS stack for a planar measurement surface. Bergler (2001) used the latter one to develop and implement the 2D CO CRS stack. In this section, I present traveltimes equations that can be used by the 2D CO CRS stack in the case of topography on the measurement surface. I will not consider velocity gradients. Moreover, I only show hyperbolic traveltimes formulas that are obtained by squaring both sides of the parabolic ones and keeping only terms up to the second order.

2D CO CRS stack for an arbitrary topography

The traveltimes formula for the 2D CO CRS stack for an arbitrary topography can directly be derived from the general moveout formula given in Zhang (2003) by setting

- the azimuth angles at the sources and receivers equal zero, i. e., $\theta_S = 0$ and $\theta_G = 0$,
- all the variables associated with the y-direction equal zero,
- and the gradients of the near surface velocity equal zero, i. e., $\nabla v(S) = 0$ and $\nabla v(G) = 0$.

The first two items are due to the fact that I consider 2D data acquisition along a straight line. Without loss of generality, I suppose it is along the x-direction. Putting these assumptions into the general traveltimes equation yields after some simple algebraic calculations the traveltimes formula for the 2D CO CRS stack for an arbitrary topography which is given by

$$\begin{aligned}
 T^2(\Delta x_S, \Delta x_G, \Delta z_S, \Delta z_G) = & \left(t_0 + \frac{\sin \beta_G}{v_G} \Delta x_G - \frac{\sin \beta_S}{v_S} \Delta x_S + \frac{\cos \beta_G}{v_G} \Delta z_G - \frac{\cos \beta_S}{v_S} \Delta z_S \right)^2 \\
 & + t_0 D B^{-1} (\Delta x_G - \Delta z_G \tan \beta_G)^2 \\
 & + t_0 A B^{-1} (\Delta x_S - \Delta z_S \tan \beta_S)^2 \\
 & - 2 t_0 B^{-1} (\Delta x_G - \Delta z_G \tan \beta_G) (\Delta x_S - \Delta z_S \tan \beta_S),
 \end{aligned} \tag{1}$$

in the hyperbolic form. A , B , and D are three elements of the surface-to-surface ray propagator matrix in a global coordinate system. Equation (1) is given in shot and receiver coordinates. By calculating the components of the 2D midpoint vector $\Delta \vec{m}$ and the 2D half-offset vector $\Delta \vec{h}$

$$\begin{pmatrix} \Delta m_x \\ \Delta m_z \end{pmatrix} = \frac{1}{2} \begin{pmatrix} \Delta x_G + \Delta x_S \\ \Delta z_G + \Delta z_S \end{pmatrix} \quad \text{and} \quad \begin{pmatrix} \Delta h_x \\ \Delta h_z \end{pmatrix} = \frac{1}{2} \begin{pmatrix} \Delta x_G - \Delta x_S \\ \Delta z_G - \Delta z_S \end{pmatrix}, \tag{2}$$

we can obtain the traveltimes formula given in Equation (1) in midpoint and half-offset coordinates. Since this equation consists of lots of terms I abstain from presenting it in this paper. Please note that Equation (1) is given in a global coordinate system. The general moveout formula in Zhang (2003) is given in a ray-centered coordinate system. Thus, to derive Equation (1), I applied a simple transformation from the ray-centered into the global coordinate system.

Zhang et al. (2001) and Bergler (2001) related the elements A , B , C , and D to three wavefront curvatures. In Bergler (2001), these curvatures are referred to as K_1 , K_2 , and K_3 where K_1 is defined as the wavefront curvature of an emerging wave at the receiver in a common-shot (CS) experiment while K_2 and K_3 are the wavefront curvatures at the source and receiver, respectively, in a (hypothetical) common-midpoint (CMP) experiment. Please note that Zhang et al. (2001) use a different notation for the wavefront curvatures. It is straightforward to calculate the traveltimes formulas in terms of wavefront curvatures in order to achieve a geometrical interpretation of all five wavefield attributes determined by the 2D CO CRS stack. In terms of

wavefront curvatures, Equation (1) reads:

$$\begin{aligned}
T^2(\Delta x_S, \Delta x_G, \Delta z_S, \Delta z_G) = & \left(t_0 + \frac{\sin \beta_G}{v_G} \Delta x_G - \frac{\sin \beta_S}{v_S} \Delta x_S + \frac{\cos \beta_G}{v_G} \Delta z_G - \frac{\cos \beta_S}{v_S} \Delta z_S \right)^2 \\
& + t_0 \Delta x_G K_1 \frac{\cos^2 \beta_G}{v_G} \Delta x_G + 2 t_0 \Delta x_S (K_1 - K_3) \frac{\cos^2 \beta_G}{v_G} \Delta x_G \\
& + t_0 \Delta x_S \left[(K_1 - K_3) \frac{\cos^2 \beta_G}{v_G} - K_2 \frac{\cos^2 \beta_S}{v_S} \right] \Delta x_S \\
& - 2 t_0 \Delta x_G K_1 \frac{\cos \beta_G \sin \beta_G}{v_G} \Delta z_G + t_0 \Delta z_G K_1 \frac{\sin^2 \beta_G}{v_G} \Delta z_G \\
& - 2 t_0 \Delta x_S \left[(K_1 - K_3) \tan \beta_S \frac{\cos^2 \beta_G}{v_G} - K_2 \frac{\sin \beta_S \cos \beta_S}{v_S} \right] \Delta z_S \\
& + t_0 \Delta z_S \left[(K_1 - K_3) \tan^2 \beta_S \frac{\cos^2 \beta_G}{v_G} - K_2 \frac{\sin^2 \beta_S}{v_S} \right] \Delta z_S \\
& - 2 t_0 \Delta x_S (K_1 - K_3) \frac{\cos \beta_G \sin \beta_G}{v_G} \Delta z_G \\
& - 2 t_0 \Delta x_G (K_1 - K_3) \frac{\tan \beta_S \cos^2 \beta_G}{v_G} \Delta z_S \\
& + 2 t_0 \Delta z_G (K_1 - K_3) \frac{\tan \beta_S \cos \beta_G \sin \beta_G}{v_G} \Delta z_S .
\end{aligned} \tag{3}$$

By setting the z-coordinates Δz_S and Δz_G in Equations (1) and (3) equal zero, we obtain the so-called conventional 2D CO CRS stacking operators for a planar measurement surface in shot and receiver coordinates as given in Zhang et al. (2001) in terms of A , B , C , and D and in Bergler (2001) and Zhang et al. (2001) in terms of wavefront curvatures, namely

$$\begin{aligned}
T^2(\Delta x_S, \Delta x_G) = & \left(t_0 + \frac{\sin \beta_G}{v_G} \Delta x_G - \frac{\sin \beta_S}{v_S} \Delta x_S \right)^2 \\
& + t_0 (\Delta x_G D B^{-1} \Delta x_G + \Delta x_S A B^{-1} \Delta x_S - 2 \Delta x_G B^{-1} \Delta x_S)
\end{aligned} \tag{4}$$

and

$$\begin{aligned}
T^2(\Delta x_S, \Delta x_G) = & \left(t_0 + \frac{\sin \beta_G}{v_G} \Delta x_G - \frac{\sin \beta_S}{v_S} \Delta x_S \right)^2 \\
& + t_0 \left[\Delta x_G K_1 \frac{\cos^2 \beta_G}{v_G} \Delta x_G \right. \\
& + \Delta x_S \left((K_1 - K_3) \frac{\cos^2 \beta_G}{v_G} - K_2 \frac{\cos^2 \beta_S}{v_S} \right) \Delta x_S \\
& \left. + \Delta x_S 2 (K_1 - K_3) \frac{\cos^2 \beta_G}{v_G} \Delta x_G \right] .
\end{aligned} \tag{5}$$

2D CO CRS stack for a smooth topography

The traveltime formulas for arbitrary topography are not well suited for a practical implementation in the framework of the CRS stack. Instead, I propose to fit a smooth topography to the real rugged one and to perform the CO CRS stack with a stacking operator that takes this smooth topography into account.

von Steht (2004) showed how to derive a ZO CRS stacking operator for smooth topography from the ZO CRS stacking operator for rugged topography. These considerations can be adopted to the CO CRS stack. Let us consider Figure 1 that shows a simple sketch of a smooth measurement surface above a single curved reflector. Moreover, a central ray SRG and a paraxial ray \overline{SRG} in the close vicinity of the central ray are

shown. We establish two local coordinate systems. The source S and the receiver R of the central ray are the origins of these coordinate systems. The two x-axes are tangent to the measurement surface at S and R, respectively, and the z-axes point in direction of the associated surface normals. We assume that the measurement surface in the vicinity of S and R can be described by parabolae:

$$z_S(x) = -\frac{K_S}{2}x_S^2 \quad \text{and} \quad z_G(x) = -\frac{K_G}{2}x_G^2. \quad (6)$$

Inserting these relationships into Equation (3) and retaining only terms up to the second order in Δx_S and Δx_G yields

$$\begin{aligned} T^2(\Delta x_S, \Delta x_G) = & \left[t_0 + \frac{\sin \beta_G}{v_G} \Delta x_G - \frac{\sin \beta_S}{v_S} \Delta x_S \right]^2 \\ & + t_0 \left[\Delta x_S 2(K_1 - K_3) \frac{\cos^2 \beta_G}{v_G} \Delta x_G \right. \\ & + \Delta x_S \left((K_1 - K_3) \frac{\cos^2 \beta_G}{v_G} - K_2 \frac{\cos^2 \beta_S}{v_S} + K_S \frac{\cos \beta_S}{v_S} \right) \Delta x_S \\ & \left. + \Delta x_G \left(K_1 \frac{\cos^2 \beta_G}{v_G} - K_G \frac{\cos \beta_G}{v_G} \right) \Delta x_G \right]. \end{aligned} \quad (7)$$

Please note that I used $z_S = \Delta z_S$, $z_G = \Delta z_G$, $x_S = \Delta x_S$, and $x_G = \Delta x_G$ in Equation (6). The emergence angles β_S and β_G are measured with respect to the surface normal at the source and the receiver of the central ray, respectively.

In order to derive the corresponding stacking operator in midpoint and half-offset coordinates, we write

$$\begin{pmatrix} \Delta x_S \\ \Delta z_S \end{pmatrix} = \begin{pmatrix} \Delta m_x - \Delta h_x \\ -\frac{K_S}{2}(\Delta m_x - \Delta h_x)^2 \end{pmatrix} \quad \text{and} \quad \begin{pmatrix} \Delta x_G \\ \Delta z_G \end{pmatrix} = \begin{pmatrix} \Delta m_x + \Delta h_x \\ -\frac{K_G}{2}(\Delta m_x + \Delta h_x)^2 \end{pmatrix}. \quad (8)$$

By replacing Δz_S and Δz_G in Equations (1) or (3) by the expressions given in Equation (8) and keeping only terms up to the second order, we can obtain the stacking operator from Equation (7) in midpoint and half-offset coordinates.

From a practical point of view, a global coordinate system is better suited for an implementation of the CRS stack. Let us consider Figure 2 in order to transform Equation (7) into a global coordinate system. It shows a smooth measurement surface with a source S. Also depicted is a local coordinate system with its origin in S and its x-axis tangent to the measurement surface in point S as well as a global coordinate system with a horizontal x-axis. The dip of the measurement surface in S is called α_S . Analogous considerations are valid for a receiver R on this measurement surface with a local dip α_R in R. From Figure 2 we obtain

$$\Delta x_S = \frac{\Delta x_S^g}{\cos \alpha_S} \quad \text{and} \quad \Delta x_G = \frac{\Delta x_G^g}{\cos \alpha_G}. \quad (9)$$

Inserting Equation (9) into Equation (7) yields the 2D CO CRS stacking operator for a smooth measurement surface in source and receiver coordinates in a global coordinate system:

$$\begin{aligned} T^2(\Delta x_S, \Delta x_G) = & \left(t_0 + \frac{\sin \beta_G}{v_G \cos \alpha_G} \Delta x_G^g - \frac{\sin \beta_S}{v_S \cos \alpha_S} \Delta x_S^g \right)^2 \\ & + t_0 \left[\frac{\Delta x_S^g \Delta x_G^g}{\cos \alpha_S \cos \alpha_G} 2(K_1 - K_3) \frac{\cos^2 \beta_G}{v_G} \right. \\ & + \frac{\Delta x_S^g \Delta x_S^g}{\cos \alpha_S \cos \alpha_S} \left((K_1 - K_3) \frac{\cos^2 \beta_G}{v_G} - K_2 \frac{\cos^2 \beta_S}{v_S} + K_S \frac{\cos \beta_S}{v_S} \right) \\ & \left. + \frac{\Delta x_G^g \Delta x_G^g}{\cos \alpha_G \cos \alpha_G} \left(K_1 \frac{\cos^2 \beta_G}{v_G} - K_G \frac{\cos \beta_G}{v_G} \right) \right]. \end{aligned} \quad (10)$$

Please note that the emergence angles β_S and β_G are still measured in the local coordinate systems, i. e., they are measured with respect to the surface normal at the source and the receiver of the central ray,

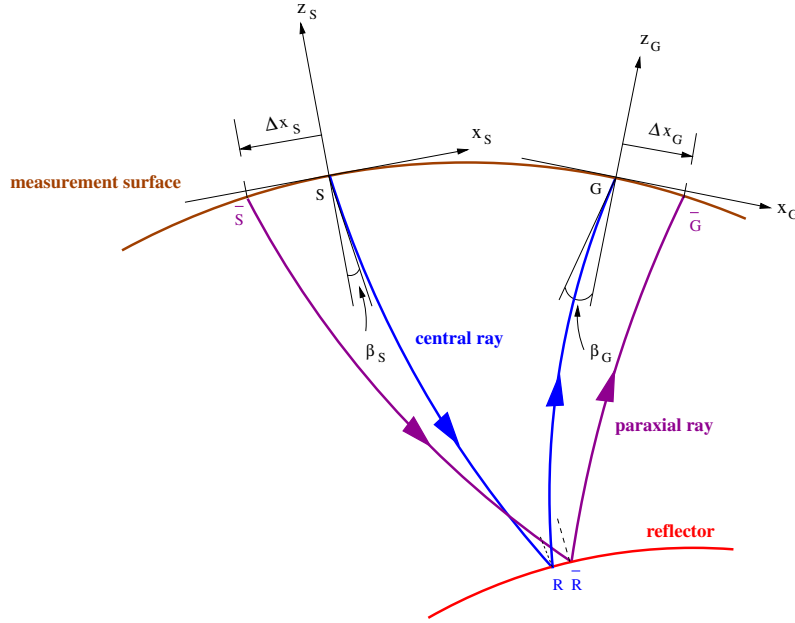


Figure 1: Local coordinate systems at source S and receiver G. See main text for details.

respectively. We can easily compute the emergence angles in a global coordinate system, β_S^g and β_G^g , by means of a rotation by the dip angles at the corresponding emergence points (see Figure 3):

$$\beta_S^g = \beta_S - \alpha_S \quad \text{and} \quad \beta_G^g = \beta_G - \alpha_G. \quad (11)$$

Please note that the minus signs in Equation (11) are due to the sign definitions of the emergence angles β_S and β_G . Setting K_S , K_G , α_S , and α_G in Equations (7) and (10) equal zero, i. e., considering a planar measurement surface, we again obtain the conventional 2D CO CRS stacking operator given in Equation (5).

In presence of a rugged top-surface topography I propose the following workflow (in analogy to the 2D ZO CRS stack):

- Topography analysis
- Elevation-static corrections
- CRS stack
- Optimization
- Redatuming

During the first step, topography analysis, a smooth topography is fitted to the real complex one. This can be done, for instance, by means of a spline interpolation. In this way, the dip and the curvature of the top-surface topography at every source and receiver location can be obtained as well as the elevation difference between the smooth surface and the complex counterpart. In the next step the sources and receivers are projected onto the determined smooth measurement surface. Since the emergence angles of the rays are not yet known, a vertical emergence is assumed. Thus, an error is introduced but the difference between the smooth and the real topography is, in general, small and, therewith, the error is small, too. There are two possibilities for the CRS stack that follows after this step. Either a stacking operator that takes the smooth topography into account can be used or the conventional one. In the latter case, the determined wavefield attributes have to be corrected afterwards if they are to be used for further analyses. Without a correction, a correct geometrical interpretation of the attributes is not possible. Later on in this paper, I will propose

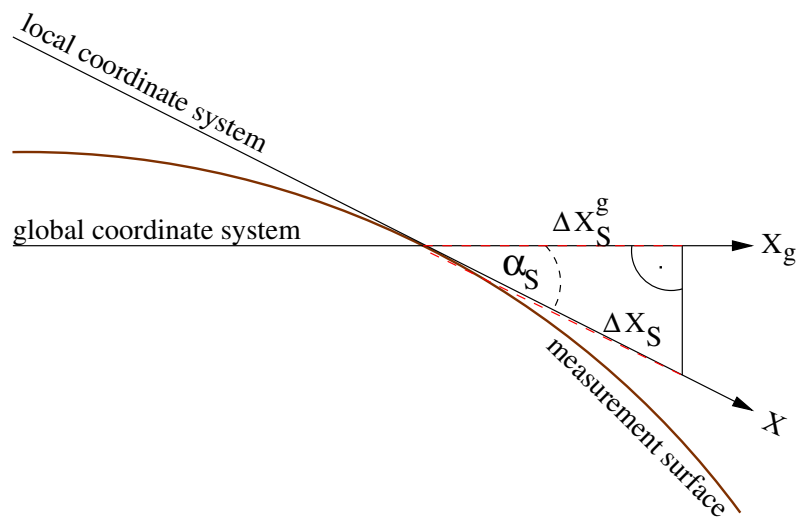


Figure 2: Global coordinate system and a local one at source S.

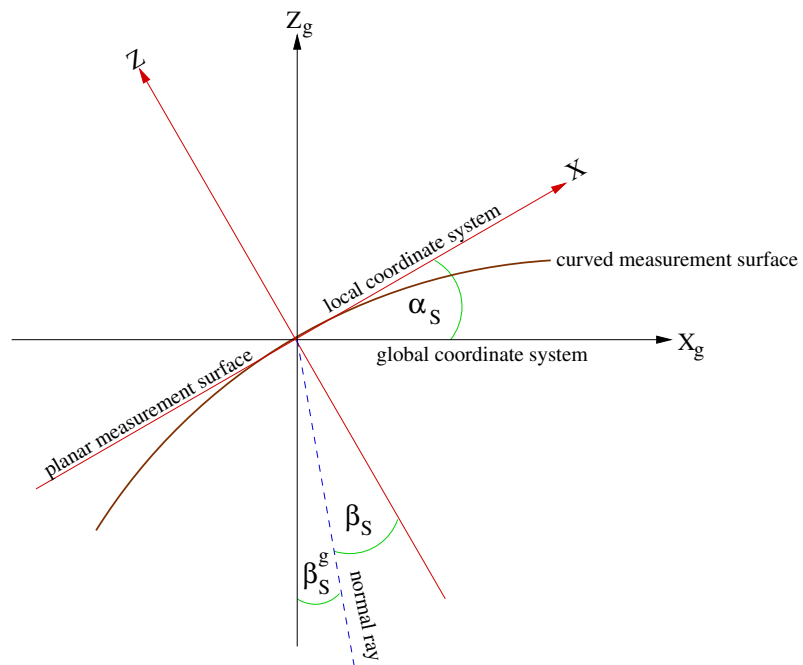


Figure 3: Rotation of β_S into a global coordinate system.

an approach how to redatum the stacked section, i. e., how to continue the central rays to a new horizontal datum line. For this purpose, the corrected emergence angles are required. By comparing Equations (10) and (5), we find the following equations to correct β_S and β_G :

$$\sin \beta_S = \cos \alpha_S \sin \beta_S^* \quad \text{and} \quad \sin \beta_G = \cos \alpha_G \sin \beta_G^* . \quad (12)$$

In Equation (12), β_S^* and β_G^* are the uncorrected emergence angles determined by the CO CRS stack. Finally, a stacking operator that considers the real complex topography can be used for an optimization of the kinematic wavefield attributes and the stacked section. For this optimization, the corrected attributes determined by the CRS stack considering a smooth topography serve as initial values. The implementation of an optimization step for the 2D CO CRS stack is currently under investigation. To get rid of the topographic footprint in the data, for instance to facilitate the interpretation of the stacked section, redatuming can be performed. I will address to this topic later on in this paper.

2D CO CRS stack for a VSP acquisition geometry

Equation (1) can be used to derive stacking operators that are applicable to VSP data. A typical 2D VSP acquisition geometry is characterized by receivers that are placed in a borehole while the sources are located along a straight line on the top-surface as for usual land seismics. VSP is also possible in marine environments. In this case, the sources (i.e. airguns) are located some meters below the water surface and the receivers are in a borehole in the solid subsurface.

Let us assume a vertical borehole and that all sources are disposed at the same level, i.e. in the same water depth or on a measurement surface on land without topography. Then, the vertical displacements between the sources, Δz_S , and the horizontal displacements between the receivers, Δx_G , vanish:

$$\Delta z_S \equiv 0 \quad \text{and} \quad \Delta x_G \equiv 0 . \quad (13)$$

Taking Equation (13) into account, Equation (3) simplifies for a VSP acquisition geometry as follows:

$$\begin{aligned} T^2(\Delta x_S, \Delta z_G) = & \left[t_0 - \frac{\sin \beta_S}{v_S} \Delta x_S + \frac{\cos \beta_G}{v_G} \Delta z_G \right]^2 \\ & + t_0 \left[\Delta x_S \left((K_1 - K_3) \frac{\cos^2 \beta_G}{v_G} - K_2 \frac{\cos^2 \beta_S}{v_S} \right) \Delta x_S \right. \\ & - 2 \Delta x_S (K_1 - K_3) \frac{\sin \beta_G \cos \beta_G}{v_G} \Delta z_G \\ & \left. + \Delta z_G K_1 \frac{\sin^2 \beta_G}{v_G} \Delta z_G \right] . \end{aligned} \quad (14)$$

This operator has in principle the same structure as the conventional 2D CO CRS stacking operator and simplifies in different subsets of the pre-stack data volume, e. g., CS and common-receiver (CR) gather. In the different subsets the stacking surface reduces to a stacking curve. Thus, the global search for the five kinematic wavefield attributes can be split up in several search routines where the maximum number of simultaneously searched-for attributes is two.

Please note that the stacking operator given by Equation (14) is valid for both VSP geometries, i. e., land and marine VSP. We consider relative displacements between the sources and receivers of central and paraxial rays. The stacking operator does not depend on the absolute depths of the receivers or sources and, thus, it is not important whether the receiver line starts at the same level of the sources or further down at the sea bottom.

Furthermore, stacking operators for so-called reverse VSP and cross-well acquisition geometries can easily be derived by means of Equation (1). In the former case, the sources are placed downhole while the receivers are deployed at the surface. Thus, we have to put Δx_S and Δz_G equal zero in Equation (1), assuming a vertical borehole and a planar and horizontal measurement surface. A cross-well acquisition means that both, sources and receivers, are placed downhole in neighboring boreholes. In this case, we have to put Δx_S and Δx_G equal zero in Equation (1), assuming vertical boreholes.

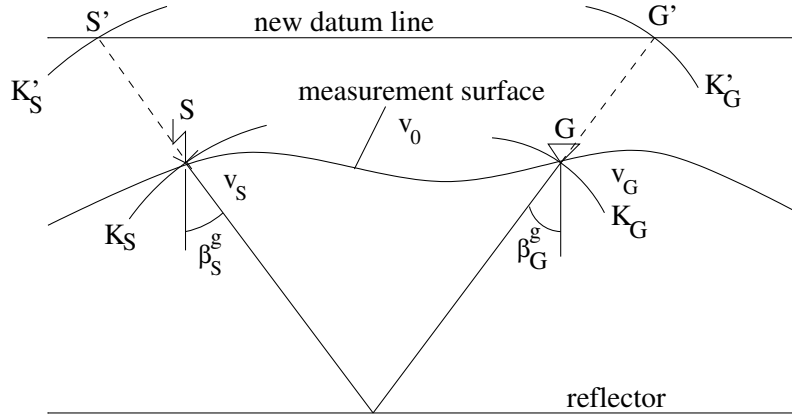


Figure 4: Redatuming of a finite-offset ray. See main text for details.

Similar considerations are valid for ocean bottom seismics (OBS) which means that the receivers are located on the ocean bottom. Assuming an ocean bottom without topography and that all sources are placed in the same water depth, the vertical displacements between the sources and between the receivers, Δz_S and Δz_G , respectively, are always equal zero. Setting these assumptions into Equation (1), we retain with the conventional 2D CO CRS stacking operator that was originally developed in order to stack data that were acquired along one straight line. For more details, I refer to Boelsen and Mann (2004) in this report.

REDATUMING

In order to get rid of the topographic influence on the data, redatuming is performed. Redatuming means that we project the sources and receivers onto a new horizontal reference level (or datum line). Since the emergence angles at the sources and receivers, β_S and β_G , respectively, are known for each central ray after the CO CRS stack, the central rays can easily be continued to the new datum line. The five wavefield attribute sections as well as the coherency section can be redatumed, too. The wavefront curvatures K_1 , K_2 , and K_3 can easily be continued, i. e., extrapolated, to the datum line by means of the *propagation and transmission law* (see Hubral and Krey, 1980). However, I will only consider the redatuming of the CO CRS stack section in this paper.

Redatuming of the stacked section

Here, the required equations to redatum the CO CRS stacked section are presented. Let us consider the simple model depicted in Figure 4. It consists of a curved acquisition line and two homogeneous layers separated by a horizontal interface. The horizontal datum line can be chosen arbitrarily. In Figure 4, it is assumed to be above the highest elevation of the measurement surface. The velocity in the fictitious layer between the acquisition and datum line is referred to as v_f . Let us consider the central ray at the receiver R. Of course, the same considerations are valid at the source S, too. The emergence angle is β_G (remember, if you choose the conventional stacking operator for the CO CRS stack you have to correct the angle by the dip of the topography at the receiver). The central ray is then refracted at the measurement line. Using Snell's law,

$$\frac{\sin \beta_G}{v_G} = \frac{\sin \beta_G^r}{v_f}, \quad (15)$$

we can calculate the refracted angle β_G^r

$$\beta_G^r = \arcsin\left(\frac{v_f}{v_G} \sin \beta_G\right). \quad (16)$$

Remember that this angle is still given in a local coordinate system. For the following considerations, we need the refracted angle in a global coordinate system. This can be achieved by using Equation (11). It is obviously convenient to assume v_f to be equal to the velocity below the acquisition line since we do not

have to consider Snell's law in this case. But nevertheless, we have to calculate the emergence angle in the global coordinate system. The vertical distance between the receiver and the new datum line is denoted as d_G . The new receiver position x'_G on the datum line can then be calculated by

$$x'_G = x_G + d_G \tan \beta_G^g. \quad (17)$$

In analogy, the new source position x'_S is given by

$$x'_S = x_S + d_S \tan \beta_S^g, \quad (18)$$

where d_S is the distance between the considered source and the datum line and β_S^g the refracted emergence angle at the source in the global coordinate system. Please note that both emergence angles can be positive or negative. Thus, the new x-positions on the datum line, x'_G and x'_S , can move to the left or the right compared to the original x-positions on the real acquisition line, x_G and x_S . Due to the continuation of the central ray to the datum line, the traveltimes is increased (assuming a datum line above the real measurement line). The additional traveltimes from the old to the new receiver position is denoted as t_G and from the old to the new source position as t_S . They are given by

$$t_G = \frac{d_G}{v_f \cos \beta_G^g} \quad \text{and} \quad t_S = \frac{d_S}{v_f \cos \beta_S^g}. \quad (19)$$

The traveltimes after redatuming is then given by

$$t'_0 = t_0 + t_G + t_S, \quad (20)$$

where t_0 is the traveltimes of the central ray from the source to the receiver on the curved measurement line. Due to redatuming, the midpoint as well as the offset of the central ray change. The new midpoint m'_x can be calculated by

$$m'_x = \frac{1}{2}(x'_S + x'_G) = m_x + \frac{1}{2}(d_G \tan \beta_G^g + d_S \tan \beta_S^g) \quad (21)$$

and the new half-offset h'_x is given by

$$h'_x = \frac{1}{2}(x'_G - x'_S) = h_x + \frac{1}{2}(d_G \tan \beta_G^g - d_S \tan \beta_S^g). \quad (22)$$

Please note that we consider only the x-components of midpoint and half-offset in the presence of a smooth acquisition line.

Implementation

The application of redatuming in the framework of the CRS stack for common-offset is more complicated than in the ZO case, since in the CO case the offset changes due to redatuming. This is not the case for the ZO CRS stack because the new source and receiver positions still coincide after redatuming. Thus, a ZO section remains a ZO section after redatuming. To solve this problem, we have to perform the CO CRS stack not only for the common-offset we are interested in but for several common-offsets in the vicinity. Then the redatuming algorithm can be applied to each sample of all CO sections and after resampling to a new grid we can obtain the redatumed CO section. In detail, the redatuming algorithm works as follows:

- Read in several CO CRS stacked sections around the CO section we want to redatum
- Choose the first sample and calculate the new traveltimes, midpoint and half-offset that correspond to an experiment that is performed on the new datum line
- Resample the new values onto a user-given grid

This has to be repeated for each sample of the input sections. When redatuming the attribute sections, we have to remember that the values of the wavefront curvatures change due to redatuming. If we choose v_f to be equal to the velocity below the measurement line, we do not have to take refraction into account and, thus, the values of the emergence angles do not change.

SYNTHETIC DATA EXAMPLE

In this section, I want to show the application of the redatuming method described in the previous section to a synthetic data set. In addition, I want to compare the data-derived emergence angles (i. e., determined by the CO CRS stack) with their exact model-derived counterparts (i. e., determined by ray tracing) since the accuracy of the determined emergence angles is important for the quality of the redatumed section.

Model

For a first test of the redatuming of a CO CRS stack section, I used the model shown in Figure 5. It consists of four homogeneous layers and a measurement surface with a smooth topography. I chose the datum line to be positioned 10 m above the highest elevation of the acquisition surface. The first reflector is horizontal in order to see whether the redatuming algorithm works properly. This reflector occurs curved in the CO CRS stacked section due to the influence of the top-surface topography but should be horizontal again after redatuming. Similarly, the second reflector with a constant dip that is curved in the stack section should no longer be curved after redatuming. For this model, a multi-coverage data set was generated. Only primary PP-reflections have been considered. Half-offsets from $h_x = 0$ km to $h_x = -1.5$ km in increments of $\Delta h_x = 0.025$ km and midpoints from $m_x = 3$ km to $m_x = 7$ km in increments of $\Delta m_x = 0.025$ m were simulated. As a seismic signal, a zero-phase Ricker wavelet of 30 Hz peak frequency was used. The sampling interval was 4 ms. Finally, random noise was added to the synthetic data set so that all CO pre-stack gathers look with respect to their signal-to-noise ratio similar to the one for half-offset $h_x = -0.25$ km (see Figure 6).

CO CRS stack results

The objective of this section is to generate a redatumed CO gather for half-offset $h_x = -0.25$ km. For this purpose, I applied the CO CRS stack not only to a half-offset $h_x = -0.25$ km but to all half-offsets in the range from $h_x = 0$ km to $h_x = -0.5$ km. The result of the CO CRS stack for $h_x = -0.25$ km is depicted in Figure 6. The signal-to-noise ratio is dramatically increased compared to the pre-stack section and all three reflectors are clearly visible. The stacking results for the other CO sections look very similar.

Comparison of data- and model-derived emergence angles

As an example, the attribute sections for the emergence angles β_S and β_G determined by the CO CRS stack for $h_x = -0.25$ km are shown in Figure 7. In this subsection, I want to show how accurate the emergence angles were determined because these two attributes are crucial for the redatuming. Since I know the model, I can calculate the exact emergence angles by means of a ray tracer. Figures 8(a) and 8(b) show the comparison between the data- (dotted) and model-derived (solid) emergence angles for all three reflectors for $h_x = -0.25$ km. The very good coincidence is clearly visible. The deviation of the data-derived attributes from the exact ones is less than one degree and mainly even less than half a degree. The comparisons for other half-offset values show very similar results. Please note that I used the conventional stacking operator. Thus, I had to correct the emergence angles β_S and β_G according to Equation (12). The required parameters for these corrections, namely the dips and curvatures of the measurement line, α_S , α_G , K_S , and K_G , were determined by means of a ray tracer which used a spline representation of the interfaces and of the measurement surface.

Redatuming result

As input for the redatuming procedure, we need the CO CRS stacked sections and the corrected emergence angle sections for all half-offset values mentioned above. The redatuming was performed as described in the previous section. The redatumed stack section for $h_x = -0.25$ km is shown in Figure 6, too. The first reflector which is horizontal in the model but occurred curved in the stacked section is now, as expected, horizontal again. In addition, the influence of the top-surface topography on the other two reflectors has vanished. This is very clearly visible for the second reflector which is not curved but less obvious for the third one since this reflector is curved in the model. The figures depicted in this section showed that the

proposed redatuming strategy works properly for the model considered here. An optimization of the determined wavefield attributes with a stacking operator for an arbitrary topography, for instance Equation (3), would probably yield more accurate attributes since the initial values are very close to the exact ones. Moreover, this could also improve the CRS stack section and the redatumed stack section. One problem with this method is that it is very time consuming to perform the CO CRS stack for so many half-offset values as it was done in this example. For real data, this strategy is probably too time consuming. In this case, it could be possible to introduce an offset binning with a larger size of the binning cells to avoid a time consuming stacking procedure for too many half-offsets.

CONCLUSIONS

In this paper, I presented new traveltime formulas for the 2D CO CRS stack that take top-surface topography into account. I considered two different types of topography, namely an arbitrary complex and a smooth topography. For both cases, I showed the hyperbolic traveltime formulas in source and receiver coordinates.

The formulas for a complex topography turned out to be not suitable for the CO CRS stack search strategy. Instead, I propose to fit a smooth measurement surface to the real one and to use a stacking operator for this smooth topography. In a final optimization step the traveltime formula for the real rugged measurement surface can be used to improve the quality of the stacked section and the accuracy of the wavefield attributes (see Heilmann and von Steht (2004) in this report for the ZO case).

Moreover, I derived a stacking operator that is able to handle a VSP acquisition geometry and discussed how to derive stacking operators for reverse VSP and cross-well seismics.

In addition, I presented a redatuming method in order to redatum the 2D CO CRS stack section to a horizontal reference datum. This is more complicated than in the ZO case since the offset changes due to redatuming in the CO case.

I applied the 2D CO CRS stack and the redatuming algorithm to a synthetic data set that was simulated with a smoothly curved measurement surface. The results showed a high-quality CO CRS stack section and accurately determined emergence angles. The proposed redatuming implementation worked properly for the model considered here: we could get rid of the topographic influence on the data. But this implementation is probably too time consuming for redatuming of real data since it requires the application of the 2D CO CRS stack to several half-offsets. In this case, I propose a more flexible offset binning.

PUBLICATIONS

Detailed results, e. g., parabolic traveltime formulas and traveltime formulas in midpoint and half-offset coordinates for the 2D CO CRS stack in the presence of top-surface topography as well as more detailed derivations of the formulas will be published in my diploma thesis in 2005.

ACKNOWLEDGMENTS

This work was kindly supported by the sponsors of the *Wave Inversion Technology (WIT) Consortium*, Karlsruhe, Germany.

REFERENCES

- Bergler, S. (2001). The Common-Reflection-Surface Stack for Common Offset - Theory and Application. Master's thesis, University of Karlsruhe.
- Heilmann, Z. (2002). The Common-Reflection-Surface Stack under Consideration of the Acquisition Surface Topography and of the Near-Surface Velocity Gradient. Master's thesis, University of Karlsruhe.
- Hubral, P. and Krey, T. (1980). *Interval velocities from seismic reflection traveltime measurements*. Soc. Expl. Geophys.
- Mann, J., Jäger, R., Müller, T., Höcht, G., and Hubral, P. (1999). Common-reflection-surface stack - a real data example. *Journal of Applied Geophysics*, 42(3,4):301-318.

Müller, T. (1999). *The Common Reflection Surface stack method – seismic imaging without explicit knowledge of the velocity model*. Der Andere Verlag, Bad Iburg.

von Steht, M. (2004). *The Common-Reflection-Surface Stack under Consideration of the Acquisition Surface Topography - Combined Approach and Data Examples*. Master's thesis, University of Karlsruhe.

Zhang, Y. (2003). *Common-Reflection-Surface Stack and the Handling of Top Surface Topography*. PhD thesis, University of Karlsruhe.

Zhang, Y., Bergler, S., and Hubral, P. (2001). Common-Reflection-Surface (CRS) stack for common-offset. *Geophysical Prospecting*, 49:709–718.

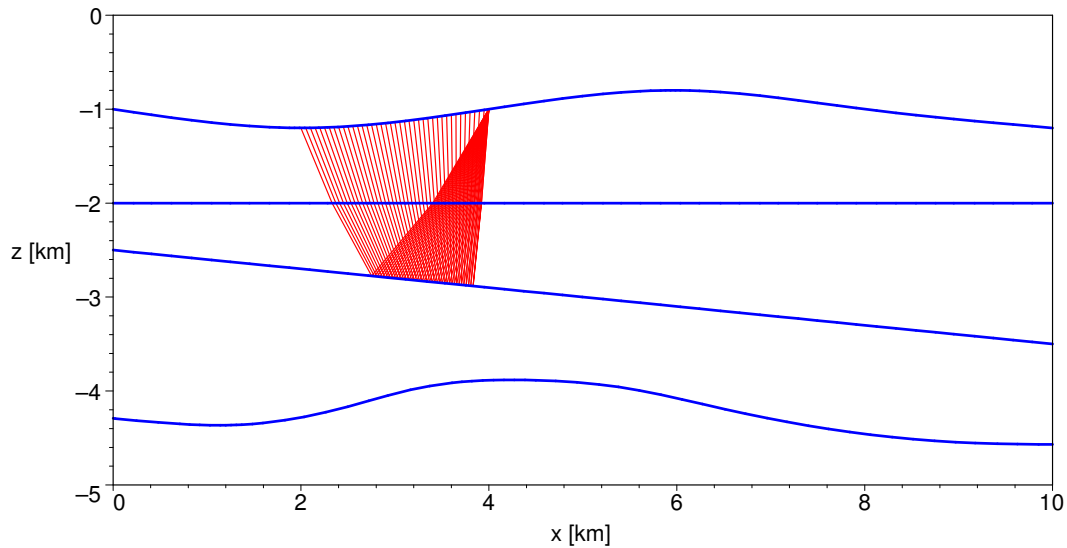


Figure 5: Model used to generate the synthetic data. To illustrate the acquisition geometry, I depicted seismic rays that are reflected at the second interface from one CS experiment.

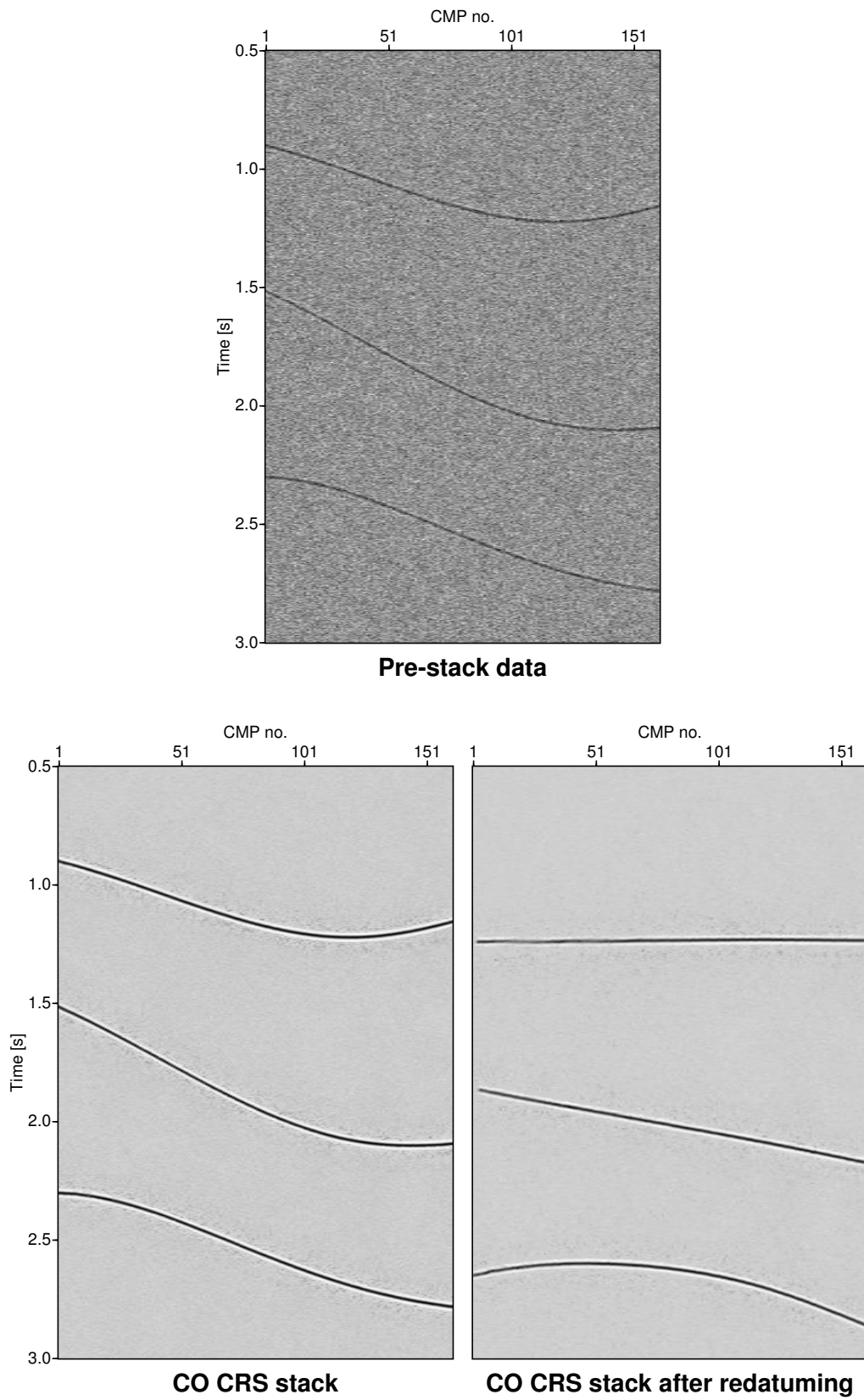


Figure 6: Pre-stack CO section ($h_x = -250$ m) for the model shown in Figure 5 and the same CO section after the CO CRS stack and redatuming.

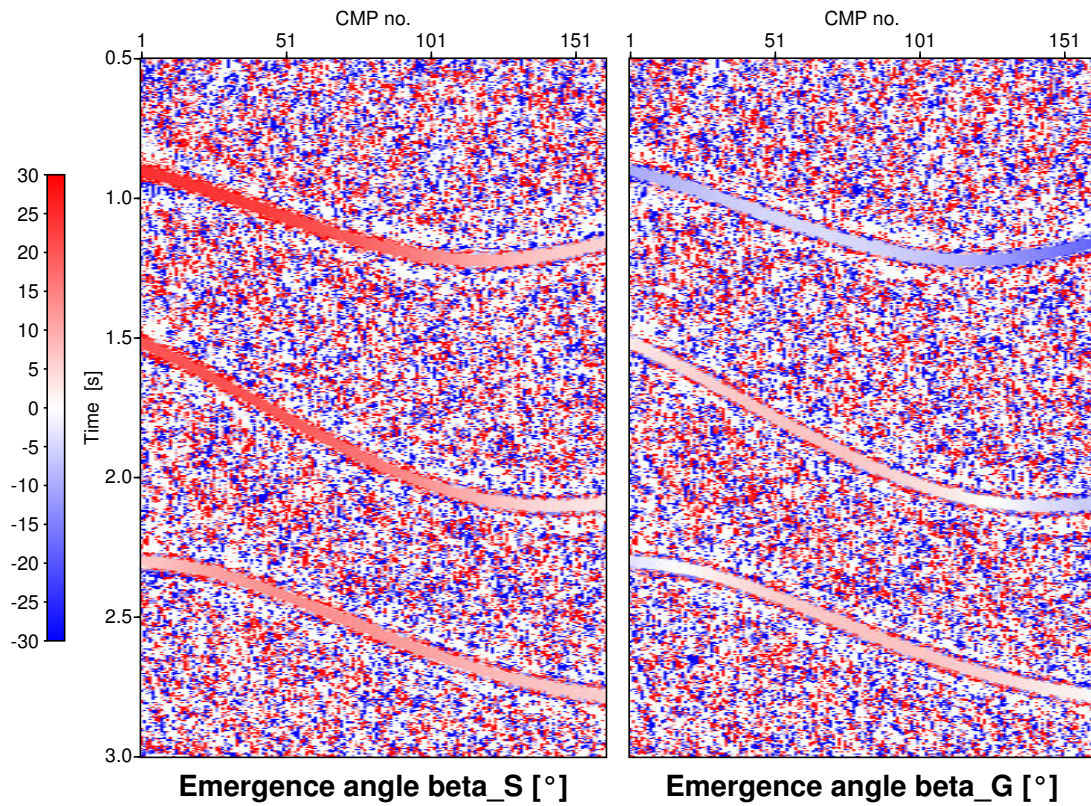
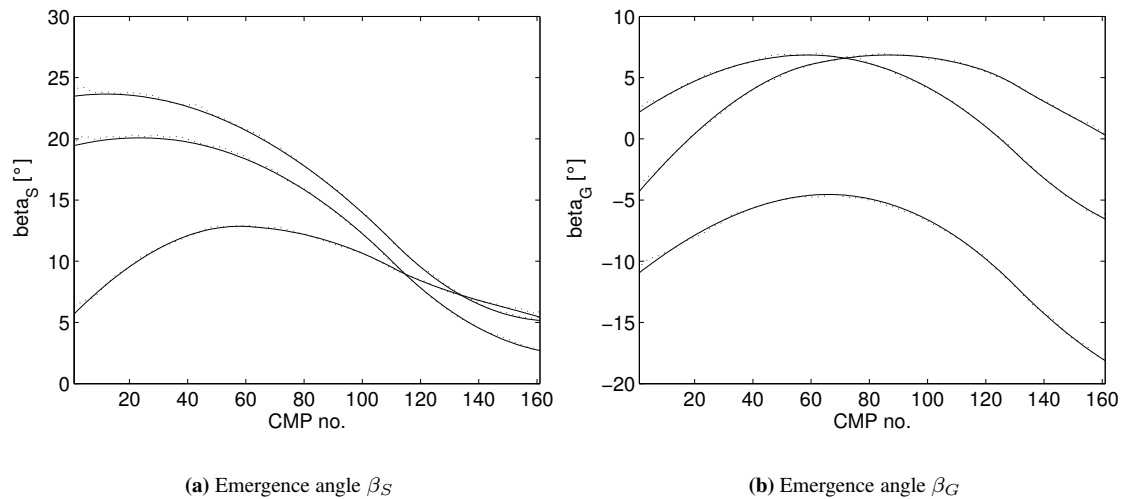


Figure 7: Emergence angles β_S and β_G ($h_x = -250$ m) determined by the CO CRS stack.



(a) Emergence angle β_S

(b) Emergence angle β_G

Figure 8: Comparison of model-derived (solid) and data-derived (dotted) emergence angles ($h_x = -250$ m).